SLOSHING MECHANICAL MODEL FOR STABILITY AND HANDLING QUALITIES EVALUATION OF THE C295 AIRCRAFT WITH THE OSD SYSTEM

Rodney Rodríguez Robles, Julián Pérez Serrano Airbus Military, Spain

Rodney.Rodriguez@military.airbus.com, Julian.Perez@military.airbus.com

Keywords: Sloshing, Simulation, Handling Qualities, Flight Test

Abstract

Airbus Military is developing a version of the C295 military aircraft with an Oil Spill Dispersant (OSD) system to be used as an airborne platform capable of dissolving marine oil spills that cause high environmental contamination and economic losses. A sloshing mechanical model was developed to evaluate the impact of the dispersant sloshing on the aircraft dynamics. Effects on aircraft stability, handling qualities and Pilot Induced Oscillations (PIO) sensitivity characteristics assessed carrying exhaustive were out simulations analyses prior to the maiden flight. Sloshing model validation was supported by Computational Fluid **Dynamics** (CFD) simulations and a dedicated flight test campaign.

This paper is structured in line with the evolution of the OSD program, starting from the development of the sloshing mechanical model and concluding with the flight test campaign results.

1 Nomenclature and abbreviations

F ForceM Moment

X Position

 Ω Angular speed

H Angular momentum

 $\overline{\overline{I}}$ Inertia tensor

f Liquid centre of gravity constraint

surface function

g Gravity acceleration vector

CG Centre of gravity

f Frequency

 θ Pitch angle

 ϕ Bank angle

m Mass

FF Fill factor of the container, defined by the ratio between the liquid volume held by the container and the volume of the

container itself

V Volume

s Arc parameter

Indexes

A "Dry" aircraft (without the liquid mass)

ACG "Dry" aircraft centre of gravity

CS Constraint surface

H HorizonL Liquid

LCG Liquid centre of gravity

LFS Liquid free-surface

Tank

2 Introduction

The sloshing phenomenon can be defined as the movement of a liquid with a free-surface inside another object (partially filled containers) that is usually undergoing motion. Different studies have emphasized the important role that liquid sloshing phenomena can play in the dynamic stability of vehicles with containers holding liquids.

The study and modelling of the convective forces and moments generated by liquid sloshing inside moving systems is of great interest to the industry, as in many occasions, in order to mitigate development risks, it is necessary to previously evaluate the impact of liquid sloshing dynamics on the overall system stability. Examples of engineering problems

were liquid sloshing is a critical issue are: cargo slosh in ships and trucks, seismic loads in containers, satellites propellant slosh under micro-gravity conditions and propellant slosh in aircrafts among others.

Within one of the C295 exportable versions, Airbus Military has integrated an oil spill dispersant system to fight against marine oil spills causing environmental disasters. Oil spill dispersants are mixtures of surface-active agents in one or more organic solvents formulated to enhance the dispersion of oil into the seawater column. Dispersants also prevent coalescence of oil droplets and re-formation of the oil slick. An aerial system for applying dispersants is essential for large spills because only aircraft can cover the oil slick area in the available time.

Forces and moments generated by the dispersant held in the OSD system tanks can be significant depending on the quantity of liquid. Dispersant sloshing impact on the C295 aircraft stability and the possible appearance of Pilot Induced Oscillations (PIO) were risk factors that needed to be precisely evaluated early in the development process. To this aim, Airbus Military has developed a sloshing mechanical model to analyse and early identify possible open/closed loop handling qualities deficiencies on the C295 with the OSD system using offline simulations. Coupled fluid and aircraft rigid body system simulations played a fundamental role on reducing uncertainties and mitigating the risks associated to the maiden flight of the OSD system.

3 The Oil Spill Dispersant System

The OSD system is a modular 6000 litre capacity aerial dispersant spray system for installation and operation from the C295 aircraft. The system comprises three tanks and a combined spray arm/pump module (Fig.1). The spray arm/pump module is installed on the ramp and the spray arms are deployed with the ramp open in horizontal position. Each tank has 2000 litre of capacity with 5% air space. Baseline configuration includes two internal baffles to diminish dispersant sloshing, dished ends and two support cradle assemblies. Tanks are fitted

to a standard cargo pallet which allows installation on the aircraft cargo handling system. System arrangement inside the cargo bay has been designed to maintain the aircraft balance within the certified CG limits at all times during the spraying operation.



Fig.1 The OSD system integrated into the Airbus DS C295 aircraft cargo bay (upper). Schematic view of the OSD system (middle). Spraying operation (bottom)

4 Liquid Sloshing Model

Forces and moments generated by liquids inside containers undergoing motion can be simulated using different methods depending on the required level of accuracy. For aircraft handling qualities assessment using online and offline simulations, liquid sloshing models based on mechanical analogies represent the best tradeoff between accuracy, model complexity, development time and required computational

budget. These models have many advantages over flow solvers that reproduce the liquid sloshing dynamics resolving the complex Navier-Stokes multi-phase equations (see [1] and [2]).

A great effort has been made to gather information about the state of the art in the mechanical models within considerably body of literature. Diverse models spring-mass and inspired on pendulum mechanical analogies have been proposed for simulating the liquid sloshing dynamics in containers with simple geometries (see [3], [4] and [5]). For containers with more complex geometries, the analytical solutions of nonviscid liquid equations cannot be derived using variables separation techniques or Rayleigh-Ritz method, and so, it is extremely difficult to obtain a first approximation of the model parameters values that define the natural frequencies of the liquid sloshing without experimental or CFD data. The sloshing mechanical model described in this paper solves much of these problems, since natural frequencies of the firsts sloshing eigenmodes are not required to be known beforehand, as they are unequivocally defined by the container geometry.

4.1 Surface Constraint Model General Description

The proposed sloshing mechanical model assumes that the CG of the dispersant mass moves along a predefined surface, hence the name of Constraint Surface Model (CSM). The proposed model considers that the liquid freesurface, which is the physical boundary between air and the liquid particles, is flat at all times. This assumption is the direct consequence of considering only the firsts sloshing linear eigenmodes neglecting the higher eigenmodes. This hypothesis is supported by the fact that the liquid energy associated to each sloshing eigenmode decays rapidly as the order of the eigenmode increases [4], thus firsts eigenmodes are sufficient to emulate the forces

and moments induced by the liquid with enough accuracy for aircraft stability and handling qualities assessments.

Basic hypotheses applied in the CSM for modelling the liquid sloshing dynamics are originally based on the analytical model proposed in [6], where the constraint surface is approximated by an equivalent ellipsoidal surface in the vicinity of the liquid CG position in order to simplify the computation of the acceleration components contained in the constraint surface tangent plane. accelerations induced by the coupled movement of the liquid-aircraft system are applied to the liquid CG, hence moving it along the elliptical surface approximation until the distance of the CG position to the actual constraint surface exceeds a tolerance value, instant when the CG position and the elliptical approximation are corrected. In the CSM, this simplified analytical approximation is not considered and the geometric constraints are solved numerically using pre-computed information of the container geometry. This new approach increases the model accuracy and allows the assessment of liquid sloshing phenomena in geometrically complex containers subjected to large amplitude excitations.

Given tank geometry, the proposed model is capable of computing an initial approach to the sloshing natural frequencies as a function of the liquid free-surface orientation and the liquid volume held in the tank. A set of internal parameters gives the model flexibility to adjust the effects of the liquid sloshing in the aircraft dynamics when experimental data or CFD simulation results are available.

4.2 Liquid CG Constraint Surfaces

Liquid CG constraint surface is the geometric locus of all possible combinations of liquid CG steady state positions given a fraction between the liquid volume and the tank volume (see Fig.2 and Fig.3). The liquid steady state conditions are calculated using the following hypothesis:

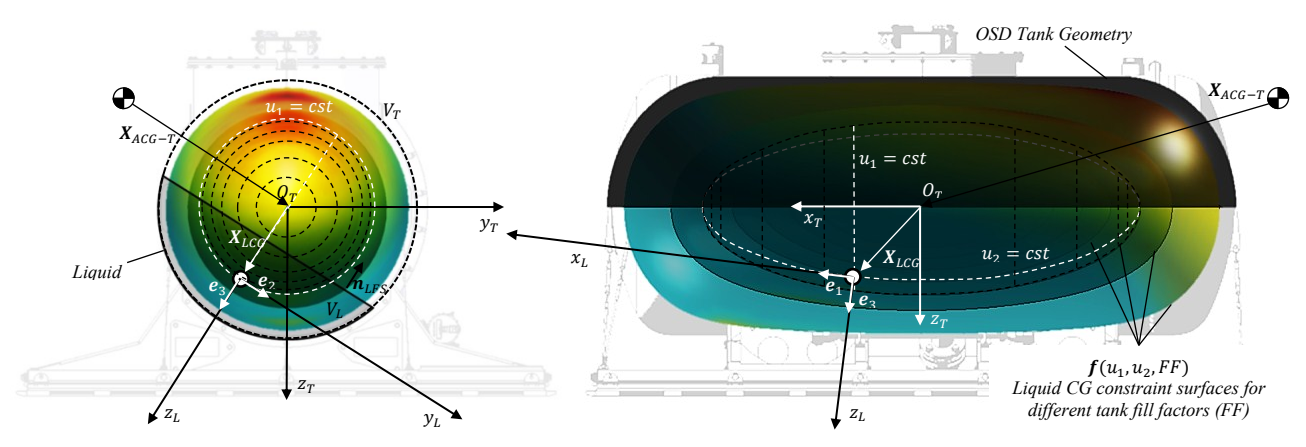


Fig.2 Schematic view of the liquid CG constraint surfaces including the variables and parameters involved in the derivation of the liquid sloshing equations

- 1. The liquid free-surface is always perpendicular to the local sensed acceleration vector.
- 2. The spatial gradient of the sensed acceleration field into the tank in steady state conditions is assumed to be zero, thus the acceleration vectors are constant into the tank volume and equal to the acceleration vector measured at the tank centre. This forces the liquid free-surface to be flat.

The aforementioned hypotheses, which apply only to steady state conditions, allow calculating the liquid CG constraint surfaces using all possible orientations of the liquid freesurface. Equations which describe the set of constraint surfaces can be derived using three parameters (i.e. two parameters associated to the surface metric and the tank fill factor):

$$\boldsymbol{X}_{CS} = \boldsymbol{f} \colon \mathbb{R}^3 \to \mathbb{R}^3 = \frac{\iiint_{V_L} \boldsymbol{X} dV}{V_T F F} = \boldsymbol{f}(u_1, u_2, FF)$$
 (1)

In addition, the normal vector of the liquid free-surface plane, and thus its orientation, is directly related to the coordinates of the liquid CG, so:

$$\mathbf{n}_{LFS} = \mathbf{h}: \mathbb{R}^3 \to \mathbb{R}^3 = \mathbf{h}(u_1, u_2, FF)$$
 (2)

For simplicity, although it is not strictly necessary, parameters u_1 and u_2 will be selected so as to define a parameterization along the principal curvature lines of the liquid CG constraint surfaces. In this way, the metric of any reference frame based on the unitary vectors $\frac{\partial f}{\partial u_1} / \left\| \frac{\partial f}{\partial u_1} \right\|$ and $\frac{\partial f}{\partial u_2} / \left\| \frac{\partial f}{\partial u_2} \right\|$ will be Euclidean

thus avoiding the use of the metric tensor in the inner products.

Complexity of the function (1) depends on containers geometry. Only for simple-shape containers this function can be derived analytically. For a generic shape container, this function needs to be solved numerically for each threesome u_1 , u_2 and FF.

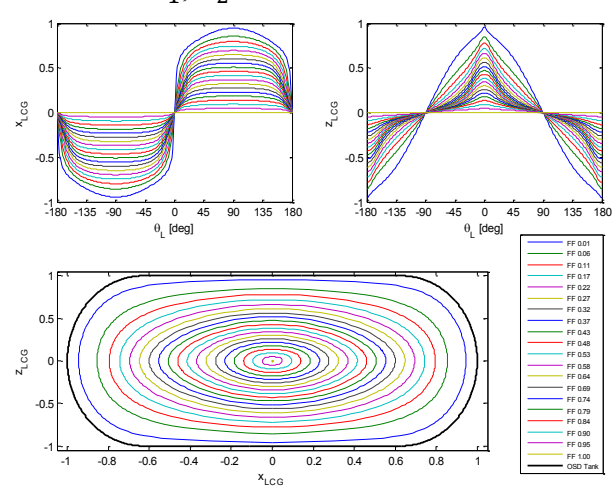


Fig.3 Vertical sections of the liquid CG constraint surfaces of the OSD tank

5 Frames of Reference

Four distinct frames of reference are used in this paper to derive the equations which describe the liquid sloshing dynamics inside each of the three tanks of the OSD system:

• Local horizon frame of reference has its origin O_H at an arbitrary point on the surface of the Earth. Its x_H axis points towards North, y_H points towards East and z_H points toward the center of the Earth.

- Aircraft body frame of reference has its origin O_A located at the "dry" aircraft CG (without the dispersant mass). Its axis x_A and z_A are parallel to the aircraft vertical plane of symmetry, being x_A parallel to the cargo bay floor. The y_A axis is perpendicular to the vertical plane of symmetry and points starboard. Finally the axis z_A points downwards so as to configure a right-handed trihedral.
- Tank frame of reference has all its axes parallel to the ones that define the aircraft body reference frame but its origin is fixed at the tanks geometric centre.
- Liquid frame of reference has its origin O_L at the instantaneous position of the liquid CG. Its x_L and y_L axes are parallel to the unit vectors $\frac{\partial f}{\partial u_1} / \left\| \frac{\partial f}{\partial u_1} \right\|$ and $\frac{\partial f}{\partial u_2} / \left\| \frac{\partial f}{\partial u_2} \right\|$ respectively. Finally, its z_L axis is parallel to $\frac{\partial f}{\partial u_1} / \left\| \frac{\partial f}{\partial u_1} \right\| \times \frac{\partial f}{\partial u_2} / \left\| \frac{\partial f}{\partial u_2} \right\|$ so as to configure a right handed trihedral.

6 Liquid Sloshing Equations of Motion

The CSM has been developed so as to ensure its compatibility and easy implementation in any kind of aircraft/vehicle simulator. To fulfil this requirement, it is necessary to separate the mechanical problem using two different mechanical sub-systems, the "dry" vehicle subsystem (without the liquid held in the tanks) and the liquid mass subsystems. In this approach, the liquid mass acts as an additional external source of forces and moments that are transmitted to the aircraft.

6.1 Momentum Equations

Momentum equations in the local horizon frame of reference are derived analysing the "dry" aircraft and the liquid subsystems separately (unless otherwise stated, all vectors are defined in the "dry" aircraft frame of reference):

$$\underbrace{m_A \frac{\mathrm{d}^2}{\mathrm{d}t^2} X_{ACG}}_{H} = \sum_{H} F_{EXT_A} + m_A g + F_L$$
(3)

$$\frac{\text{Liquid subsystem}}{m_L \frac{d^2}{dt^2} (X_{ACG} + X_{ACG-T} + X_{LCG}) \Big|_{H}} = m_L \mathbf{g} - \mathbf{F}_L$$
(4)

To expand momentum equation (4), the different acceleration terms shall be analysed separately:

$$\frac{\mathrm{d}^2}{\mathrm{d}t^2} X_{ACG} \bigg|_{H} = \frac{\mathrm{d}^2}{\mathrm{d}t^2} X_{ACG} \bigg|_{A} + \Omega_A \times \frac{\mathrm{d} X_{ACG}}{\mathrm{d}t} \bigg|_{A}$$
 (5)

$$\frac{\mathrm{d}^{2}}{\mathrm{dt}^{2}} \mathbf{X}_{ACG-T} \bigg|_{H} = \mathbf{\Omega}_{A} \times \mathbf{\Omega}_{A} \times \mathbf{X}_{ACG-T} + \frac{\mathrm{d}\mathbf{\Omega}_{A}}{\mathrm{dt}} \bigg|_{A} \times \mathbf{X}_{ACG-T} \tag{6}$$

Last acceleration term of equation (4) shall be compatible with constraints of equation (1) to ensure the liquid CG keeps at all times within the constraint surface:

$$X_{LCG}(t) = X_{CS} = f(u_1(t), u_2(t), FF(t))$$
 (7)

$$\frac{d^{2}}{dt^{2}} \boldsymbol{X}_{LCG} \bigg|_{H} = \frac{d^{2}}{dt^{2}} \boldsymbol{X}_{LCG} \bigg|_{A} + \boldsymbol{\Omega}_{A} \times \boldsymbol{\Omega}_{A} \times \boldsymbol{X}_{LCG} + \left(\frac{d\boldsymbol{\Omega}_{A}}{dt}\right|_{A}\right) \times \boldsymbol{X}_{LCG} + 2\boldsymbol{\Omega}_{A} \times \frac{d}{dt} \boldsymbol{X}_{LCG} \bigg|_{A}$$
(8)

$$\frac{\mathrm{d}^{2}}{\mathrm{dt}^{2}}X_{LCG}\Big|_{A} = \frac{\partial^{2} \mathbf{f}}{\partial u_{1}^{2}}\dot{u}_{1}^{2} + \frac{\partial \mathbf{f}}{\partial u_{1}}\ddot{u}_{1} + \frac{\partial^{2} \mathbf{f}}{\partial u_{2}^{2}}\dot{u}_{2}^{2} \qquad (9)$$

$$+ \frac{\partial \mathbf{f}}{\partial u_{2}}\ddot{u}_{2} + \frac{\partial \mathbf{f}}{\partial FF^{2}}\ddot{F}F + \frac{\partial \mathbf{f}}{\partial FF}F^{2}$$

$$+ 2\left(\frac{\partial^{2} \mathbf{f}}{\partial u_{1}\partial u_{2}}\dot{u}_{1}\dot{u}_{2} + \frac{\partial^{2} \mathbf{f}}{\partial u_{1}\partial FF}\dot{u}_{1}FF + \frac{\partial^{2} \mathbf{f}}{\partial u_{2}\partial FF}\dot{u}_{2}FF\right)$$

Terms related to *FF* variations in equation (9) can be neglected due to:

- The problem is considered to be quasistationary during the dispersant discharges.
- The magnitude orders of the tanks fill factor terms are much smaller than the magnitude order of the convective terms associated to the liquid CG movement during dispersant discharges.

Differential equations (4) need to be rewritten in the liquid frame of reference to facilitate the physical interpretation of the various terms that appear in the equations, more specifically, the dissipative terms associated to the liquid viscosity and turbulence.

Multiplying equation (4) by the orthogonal unit vectors of the surface coordinate system e_i and using the transformation matrix \overline{T}_{LA} , finally the equations of motion of the liquid CG in the constraint surface sub-space can be derived:

$$\mathbf{e}_{i} = \frac{\partial \mathbf{f}}{\partial u_{i}} / \left\| \frac{\partial \mathbf{f}}{\partial u_{i}} \right\|_{I} \tag{10}$$

$$e_{i}\overline{T}_{LA}\frac{\mathrm{d}^{2}}{\mathrm{d}t^{2}}(X_{ACG} + X_{ACG-T} + X_{LCG})\bigg|_{H}$$

$$= e_{i}\overline{T}_{LA}(g - F_{L}/m_{L})$$
(11)

$$\ddot{u}_{i} = \left(\boldsymbol{e}_{i}\overline{\boldsymbol{T}}_{LA}\frac{\partial \boldsymbol{f}}{\partial u_{i}}\right)^{-1} \left\{-\boldsymbol{e}_{i}\overline{\boldsymbol{T}}_{LA}\frac{\mathrm{d}^{2}}{\mathrm{d}t^{2}}(\boldsymbol{X}_{ACG}) + \boldsymbol{X}_{ACG-T}\right\}_{H} + \boldsymbol{e}_{i}\overline{\boldsymbol{T}}_{LA} \left[\left(\boldsymbol{g} - \boldsymbol{F}_{L} / m_{L}\right) - \boldsymbol{\Omega}_{A} \times \boldsymbol{\Omega}_{A} \times \boldsymbol{X}_{LCG} - \frac{\mathrm{d}\boldsymbol{\Omega}_{A}}{\mathrm{d}t}\right]_{A} \times \boldsymbol{X}_{LCG} - 2\boldsymbol{\Omega}_{A} \times \left(\frac{\partial \boldsymbol{f}}{\partial u_{1}}\dot{u}_{1} + \frac{\partial \boldsymbol{f}}{\partial u_{2}}\dot{u}_{2}\right) - \frac{\partial^{2}\boldsymbol{f}}{\partial u_{1}^{2}}\dot{u}_{1}^{2} - \frac{\partial^{2}\boldsymbol{f}}{\partial u_{2}^{2}}\dot{u}_{2}^{2} - 2\frac{\partial^{2}\boldsymbol{f}}{\partial u_{1}\partial u_{2}}\dot{u}_{1}\dot{u}_{2}\right\}$$

i = 1,2

Terms $e_i \overline{T}_{LA} F_L / m_L$ in (12) represent the dissipative acceleration induced by the liquid viscosity and turbulence in the directions e_1 and e_2 . In general, these dissipative terms can be modelled as follows:

$$\mathbf{e}_{i}\overline{\mathbf{T}}_{LA}\mathbf{F}_{L}/m_{L} = D_{i}(u_{i}, \dot{u}_{i}, FF)\dot{u}_{i}; \quad i = 1,2$$
 (13)

Where D_i is a non-linear function that depends on the tank fill factor and on the position and speed of the liquid CG.

Differential equations (12) provide the mathematical frame necessary to solve the

mechanical analogy of the liquid sloshing problem using simplifying hypotheses. Once the evolution of the liquid CG has been obtained, the liquid forces transmitted to the aircraft through the tank walls are computed using equation (4).

6.2 Angular Momentum Equations

Moments M_L generated by the liquid pressure and the shear stress distributed on the wetted container walls will be calculated using the angular momentum equations formulated in the local horizon frame of reference. Unless otherwise stated, all vectors appearing in the following equations are defined in the "dry" aircraft frame of reference:

$$\frac{\frac{\mathrm{d}}{\mathrm{dt}}(\bar{I}_{A}\Omega_{A})\Big|_{H}}{\left|\sum_{H} \mathbf{M}_{EXT_{A}} + \mathbf{M}_{L}\right|}$$
(14)

$$\underbrace{\frac{\mathrm{d}}{\mathrm{dt}} H_L \Big|_{H}}_{Liquid subsystem} = m_L (X_{ACG-T} + X_{LCG}) \times \mathbf{g}$$

$$-\mathbf{M}_L - m_L Y_{ACG} \times Y_{LCG}$$
(15)

$$H_{L} = m_{L}(X_{ACG-T} + X_{LCG}) \times \frac{\mathrm{d}}{\mathrm{dt}}(X_{ACG} + X_{ACG-T} + X_{LCG})\Big|_{H} + \bar{I}_{L}\Omega_{L}$$
(16)

Expanding (15, 16) and solving M_L :

$$M_{L} = (X_{ACG-T} + X_{LCG}) \times F_{L} + \overline{I}_{L} \frac{d}{dt} \Omega_{L} \Big|_{A}$$

$$+ \left(\frac{d}{dt} \overline{I}_{L} \right) \Omega_{L} + \Omega_{L} \times \overline{I}_{L} \Omega_{L}$$
(17)

Where \overline{I}_L is the equivalent inertia tensor of the liquid mass computed at the instantaneous liquid CG taking into account the liquid free-surface orientation.

$$\bar{I}_L = I(u_1(t), u_2(t), FF(t))$$
 (18)

$$\frac{\mathrm{d}}{\mathrm{dt}}\bar{I}_{L} = \frac{\partial I}{\partial u_{1}}\dot{u}_{1} + \frac{\partial I}{\partial u_{2}}\dot{u}_{2} + \underbrace{\frac{\partial I}{\partial FF}\dot{F}F}_{Negliaible}\dot{F}F$$
(19)

Inertia tensor mathematical definition only has valid physical meaning with the rigid body assumption. Applying the rigid body angular momentum equations to processing non-rigid systems can result in wrong physics results, thus the classical formulation of the rigid body inertia tensor shall be corrected to account for the fluid convective effects.

Liquid inertia tensor concept is useful in the simplifying assumption of inconsequential coupling between the rotation of the container and the fluid in certain directions, which means that depending on containers geometry, some of the fluid moment of inertia terms can be neglected. Analytical solutions have been proposed to calculate the inertia tensor of a liquid held in containers with simple geometries [7]. These solutions require the liquid sloshing eigenmodes to be known beforehand, which is not always possible. In the CSM, the equivalent liquid inertia tensor is computed using the rigid body tensor in combination with adjustable inertia correction factors.

7 Liquid Dissipative Functions

Functions $D_1(u_1, \dot{u}_1, FF)$ and $D_2(u_2, \dot{u}_2, FF)$ in (13) represent a model of the dissipative forces generated by the liquid viscosity and turbulence effects. The simplest model of dissipative sources is a linear one which induces forces or accelerations that are proportional to the speed $(D_1 = C_1 \text{ and } D_2 = C_2)$. This assumption is valid for low-amplitude liquid CG oscillations, nevertheless in the high-amplitude regime, dissipative terms no longer can be assumed to be linear [5]. Wave breaking phenomena and the increment of the turbulence intensity inside the flow field sharply increase the dissipation rate of the liquid energy.

To model both linear and non-linear dissipation effects, the following piecewise function has been implemented in the CSM:

$$D_i = D_{0i} + D_{1i}(\dot{u}_i - G_i)^2 H(|\dot{u}_i - G_i|)$$

$$i = 1,2$$
(20)

Where H is the Heaviside step function and D_{1i} and G_i are user defined parameters that can be adjusted using experimental data.

8 Liquid Sloshing Natural Frequencies

Natural frequencies of the firsts liquid sloshing eigenmodes provided by the CSM in the linear regime can be derived using the local curvature of the liquid CG constraint surface and the magnitude of the sensed acceleration component which is parallel to the surface normal vector. Using an auxiliary arc-length surface parameterization and considering the tank subjected only to gravity acceleration, the firsts liquid sloshing natural frequencies can be derived using the main curvatures of the surface κ_{u1} and κ_{u2} like:

$$s_i = \int \left\| \frac{\partial \mathbf{X}_{CS}}{\partial u_i} \right\| du_i = S_i(u_1, u_2, FF); \quad i = 1, 2 \quad (21)$$

$$\omega_{1u_i} = \sqrt{e_3 g \kappa_{ui}} = \sqrt{e_3 g \left\| \frac{\partial e_i}{\partial s_i} \right\|}; \quad i = 1,2 \quad (22)$$

Fig.4 depicts the solution of equations (22) for the OSD tank geometry for different *FF* values and tank pitch angles.

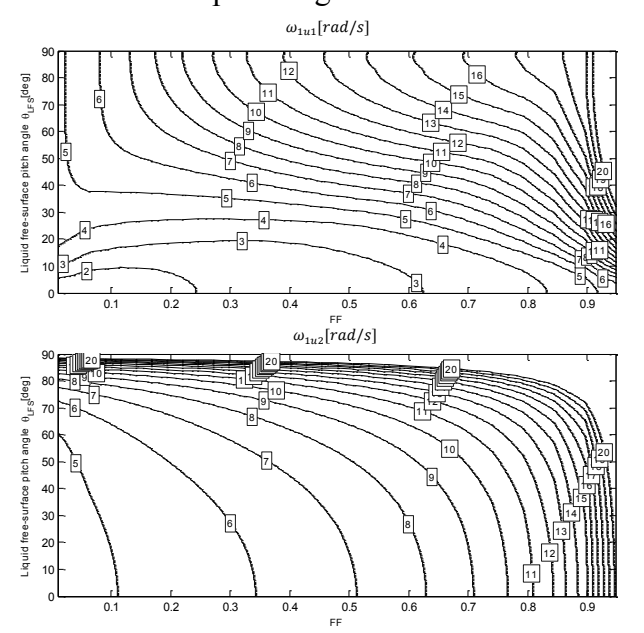


Fig.4 Liquid sloshing natural frequencies ω_{1u_1} and ω_{1u_2} in the OSD tank (1G case)

As suggested by equation (22), it is possible to artificially adapt the value of these frequencies by locally modifying the constraint surface curvature. To this aim, different adjustable geometrical factors have been added to the CSM to proportionate certain flexibility

during the model validation and adjustment process supported by experimental data.

9 Pre-Flight Validation with CFD Simulations

As part of the risk mitigation program scheduled before the maiden flight of the OSD system, CFD simulations contributed to partially validate the liquid slosh dynamics predicted by the CSM thus reducing uncertainties associated to the lack of experimental data. Much of these uncertainties were related to the dissipative characteristics of the dispersant and the effects of the baffles in the liquid sloshing dynamics.

A matrix of CFD experiments was elaborated for the pre-flight validation to identify and verify the sloshing dynamics within the target envelope of the CSM. Experiments were designed so as to provide sufficient data for the identification tasks with the minimum number of experiment configurations. A total number of 22 CFD simulations tests composed of a combination of different longitudinal and lateral acceleration profiles, *FF* values and tank attitudes were carried out.

CFD simulations allowed to identify various liquid nonlinear phenomena and contributed to adjust the dissipative functions stated in (20). It was noticed that the thresholds values G_i in (20) decayed with the liquid freesurface pitch angle θ_{LFS} , which means that the appearance of nonlinearities in the dissipative terms anticipate as the OSD tank is oriented vertically.

In addition, it was found that the liquid inertia tensor in experiments with partially empty tanks (FF \cong 0) had negligible effects on the momentum equations. On the contrary, for liquid volumes close to the tank maximum capacity (FF \cong 1), the liquid inertia tensor had to be corrected to match the moments of the CFD simulations. In these cases, the angular acceleration of the liquid free surface does not induce the movement of the whole liquid mass. This intuitive idea means that, when the aircraft is in a quasi-stationary condition $\left(\frac{d}{dt}\Omega_{AH}\right|_{H}\cong\mathbf{0}$),

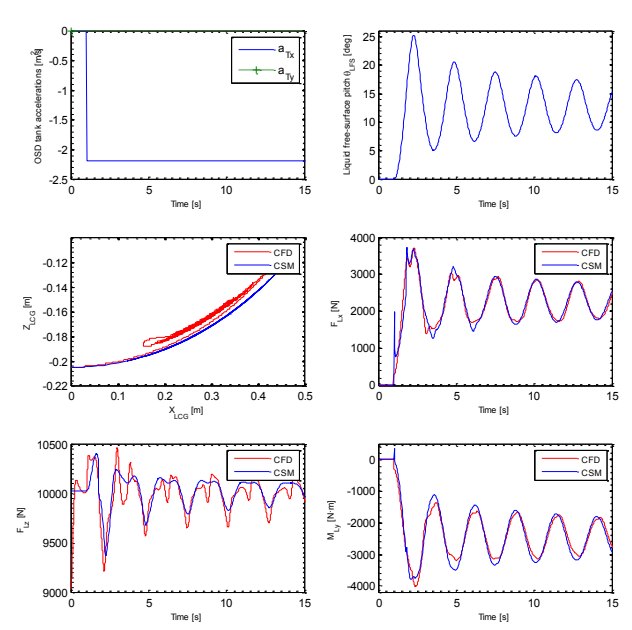


Fig.5 Longitudinal acceleration test comparing CFD and CSM results

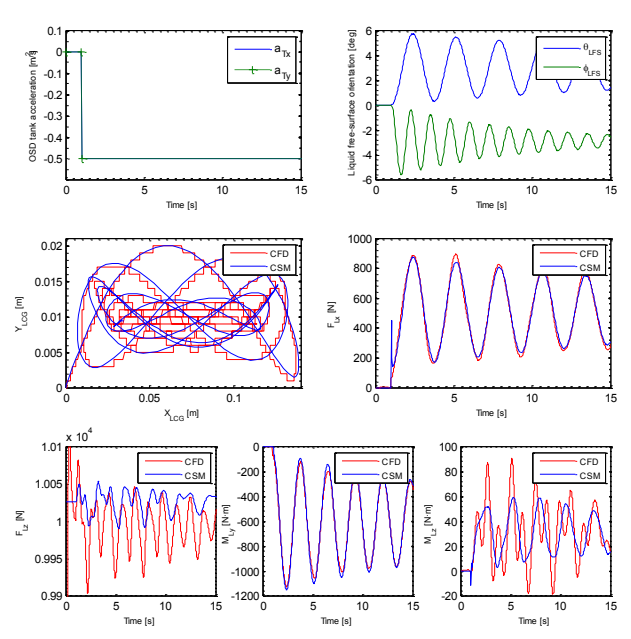


Fig.6 Lateral and longitudinal low amplitude acceleration test comparing CFD and CSM results

the movement of the air bubble inside the tank only induces accelerations on the liquid particles located near its vicinity, so the "solidequivalent" movement occurs with a much smaller amount of liquid mass.

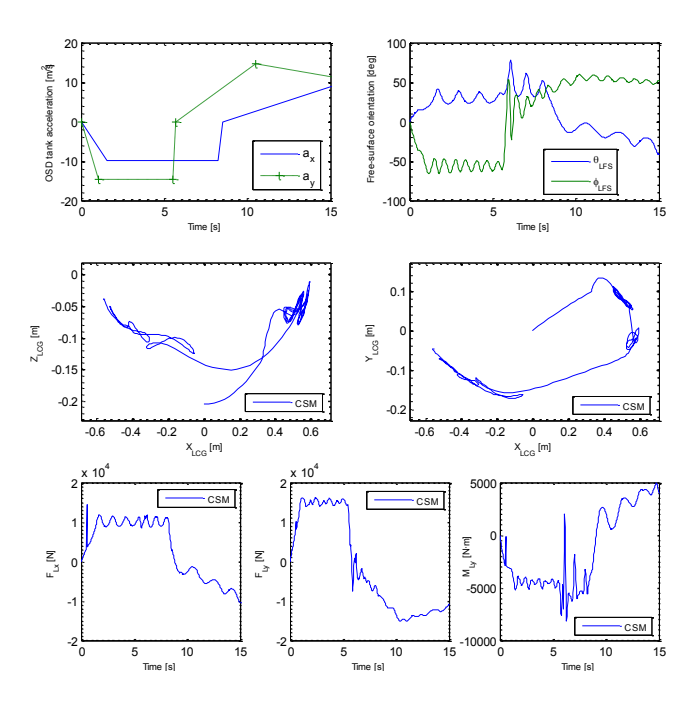


Fig.7 Liquid dynamic response to a generic high amplitude excitation

Comparisons between CSM predictions and CFD simulation results have been depicted in Fig.5 and Fig.6 for two different experiments. Fig.5 corresponds to a 0.25Gs longitudinal acceleration test with FF = 0.5. On the other hand, Fig.6 depicts a combined longitudinal and acceleration test with FF = 0.5lateral specifically designed to analyse the low amplitude liquid sloshing characteristics. Fig.7 depicts the liquid response to a generic high amplitude excitation showing also the complex trajectory shape described by the liquid CG and the high nonlinearity of its dynamics with rapid changes on the oscillation frequencies.

10 CSM Integration in the C295 Engineering Simulator

Three independent modules of the CSM (one for each OSD tank) were integrated in the C295 engineering simulator, to develop a coupled fluid and rigid body dynamics solver. As depicted in Fig.8 and Fig.9, simulator structure was adapted to integrate the forces and moments generated by each of the CSM modules along with the aerodynamic, engine and undercarriage forces and moments.

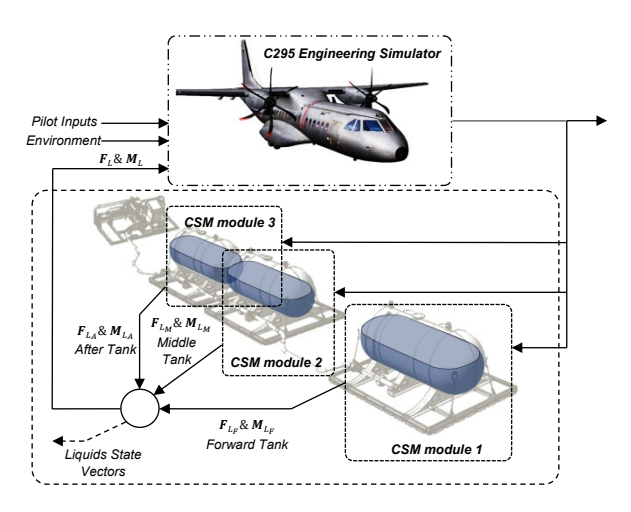


Fig.8 Data flow of the coupled fluid and rigid body dynamics solver

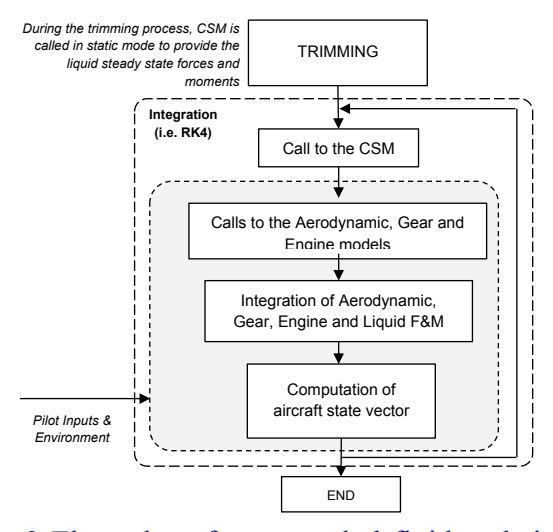


Fig.9 Flow chart for a coupled fluid and rigid body dynamics solver

11 Offline Simulations Analyses

carried Analyses out based were on comparisons between the stability and controllability characteristics of the C295 with OSD system and the basic C295 stability and controllability characteristics with equivalent mass-CG settings (reference). Flight conditions and manoeuvres were selected taking into account worst cases from flying qualities perspective using the experience acquired in previous flight test campaigns.

The liquid-frozen reference configuration was constructed from the aircraft trimmed condition. During the simulations, the liquid forces and moments of the reference cases were the same as the ones generated by a fixed

fictitious mass located at the trimmed liquid CG position. Results for this reference configuration were compared with simulations that included the full liquid sloshing effects.

Minor differences were observed on the offline simulations results for open loop manoeuvres. Deviations from the reference configuration were induced by the liquid sloshing forces and moments which resulted to be small in comparison with the magnitude of the forces and moments generated by the aircraft aerodynamics, the power plant and the undercarriage.

Regarding closed loop manoeuvres, it was noticed that in calm air conditions, depending on tanks fill factor, the low amplitude accelerations induced by the liquid sloshing might slightly augment the pilot workload to achieve high precision tasks. Critical tanks fill factor was found to be 0.7.

Offline simulation results demonstrated that trimmability, controllability and stability characteristics of the C295 with the OSD system for any tank fill factor were notionally as for C295 basic configuration. No safety issue was detected during this phase and thus, from the flying qualities point of view, the aircraft was cleared for the maiden flight of the OSD system and the posterior flight test campaign.

12 Post-Flight Model Validation with Flight Test Data

Prior to the C295 handling qualities certification flight test campaign, it was scheduled a development flight test campaign with the following objectives:

- 1. Validate the liquid sloshing simulation model Early identify possible closed loop handling qualities deficiencies not detected in the offline simulations
- 2. Evaluate if baseline baffles configuration provides the required sloshing damping

Tests were carried out with one instrumented tank located in the rearward part of the aircraft cargo bay without the pump module and the hoses that connect the tanks.

12.1 Flight Test Instrumentation

Specific flight test instrumentation was required to measure the liquid sloshing dynamics inside the OSD tank. The need to use nonintrusive instrumentation conditioned the selection of an instrumentation configuration that could measure the liquid movement in an indirect way. Finally adopted solution consisted of a total of four biaxial strain gauges positioned symmetrically at the maximum deformation locations in the tank attachment structure (see Fig.10).

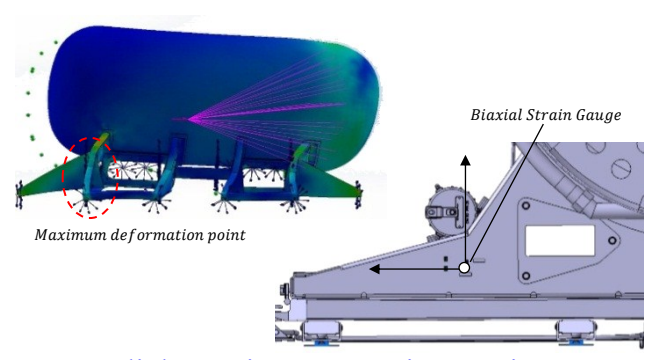


Fig.10 Flight test instrumentation: strain gauges locations

With this configuration, the local deformations measured in orthogonal directions can be post processed so as to obtain an indirect measure of the longitudinal-lateral frequencies and the damping of the convective forces generated by the liquid during the identification manoeuvres (strain gauges were not required to be calibrated).

12.2 Flight Test Campaign

Flight test campaign was divided into a set of handling qualities manoeuvres using a conservative build-up approach, starting from FF = 0.25 tests to end with FF = 0.75 tests.

Open-loop manoeuvres were selected according to available data from pervious flight test campaigns of the basic C295 so as to measure possible handling qualities discrepancies induced by the liquid sloshing. During these tests, aircraft dynamic modes (i.e. phugoid, short period, etc.) were excited separately with dedicated manoeuvres.

In parallel, liquid sloshing impact on aircraft susceptibility to PIOs was assessed with

dedicated close-loop manoeuvres, including approaches and go-around manoeuvres, crosswind landings, bank to bank and heading captures among others.

Different automatic manoeuvres were tested to assess possible non detected coupling of the liquid sloshing dynamics with the aircraft Auto-Pilot modes. These manoeuvres consisted on auto-landings, heading captures, altitude and speed acquisitions and holding patterns.

Besides performing manoeuvres, pilot's main task was to identify and give feedback of any kind of issue or difference performing the manoeuvres due to the liquid held in the OSD tank. As summary of the pilot evaluation, no differences regarding basic C295 identified during the execution manoeuvres, thus as it was expected, no noticeable effect on the aircraft handling qualities and Auto-Pilot performances could be attributed to the liquid sloshing. Comparative flight test results for aircraft phugoid and Dutchroll modes are depicted in Fig.11, where slight period discrepancies can be observed (dimensionless periods).

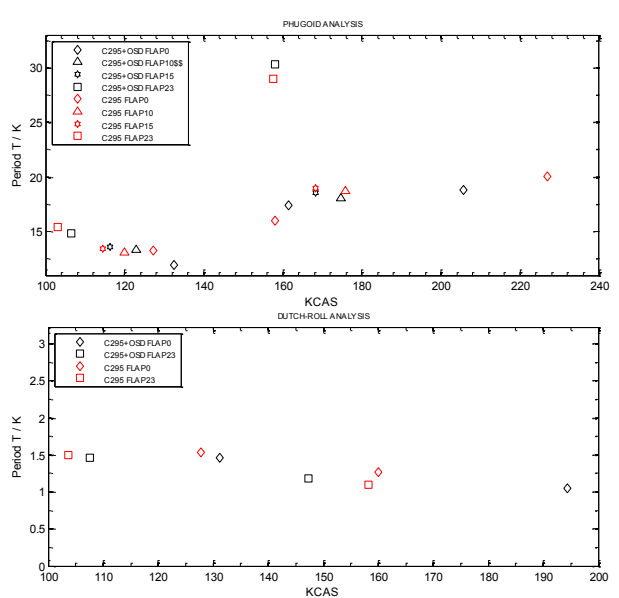


Fig.11 Aircraft eigenmodes periods computed using flight test data comparing the basic C295 aircraft with the C295+OSD system @ FF = 0.5

Regarding CSM post-flight validation, two different approaches were applied. First, flight test manoeuvres were reproduced using the C295 engineering simulator coupled with the CSM. Results were compared with the flight test data. Second, dynamic characteristics of strain gauges measurements (only the oscillation frequencies and the damping were required to be validated) were compared with the ones of the liquid sloshing forces predicted by the CSM using the flight test data to feed the model (see Fig.12).

Flight test instrumentation measurements and in-tolerance re-predictions results provided sufficient evidences to fully validate the CSM and certify that it fulfils the required level of accuracy to reproduce the liquid sloshing dynamics inside each of the three tanks of the OSD system integrated in the C295 aircraft.

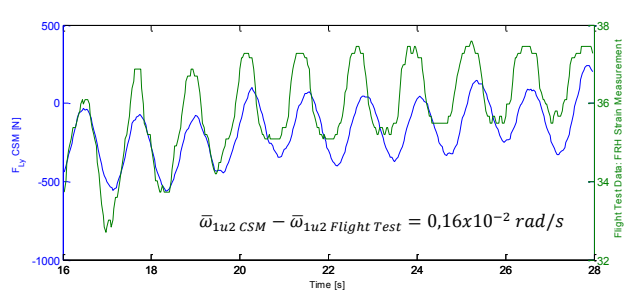


Fig.12 Comparative example depicting flight test and CSM predicted results showing the good frequency matching for ω_{1u2} @ FF = 0.25

Conclusions

The Constraint Surface Model has demonstrated to be a versatile and powerful simulation tool capable of predicting with fair accuracy the liquid sloshing dynamics in geometrically complex containers undergoing motion.

Model validation through CFD simulations remains still necessary when it is required to determine with precision the wide variety of liquid nonlinear phenomena that appear in the high amplitude excitations regime. CFD simulations carried out as part of the risk mitigation program permitted to identify the particular liquid sloshing dynamics in the OSD tanks. Results were used to enhance the CSM accuracy which contributed to lower the uncertainties affecting the flight test campaigns and to diminish the number of flight tests required to fully validate the model.

Data gathered during the reduced flight test campaign and manoeuvres re-predictions using offline simulations demonstrated that the sloshing mechanical model fulfilled the required level of fidelity to reproduce the liquid sloshing dynamics inside each tank of the OSD system.

In conclusion, it can be stated that the CSM supposed a major breakthrough in the ability to evaluate the impact of liquid sloshing in the handling qualities of the C295 aircraft equipped with the OSD system.

References

- [1] Takehiro Himeno, Yutaka Umemura and Toshinori Watanabe and Hiroshi Aoki. *Preliminary investigation on heat exchange enhanced by sloshing*. American Institute of Aeronautics and Astronautics Joint Propulsion Conference & Exhibit, Hartford, AIAA 2008-4550, 2008.
- [2] Hamid Alemi Ardakani and Thomas J. Bridges. Shallow-water sloshing in containers undergoing prescribed rigid-body motion in three dimensions. Journal of Fluid Mechanics, Vol. 667, pp 474-519, 2011.
- [3] Ibrahim R. A. *Liquid sloshing dynamics: theory and applications*. Cambridge University Press, 2005.
- [4] S. Papaspyrou, D. Valougeorgis, S. A. Karamanos. Sloshing effects in half-full horizontal cylindrical containers under longitudinal excitation. Journal of Applied Mechanics, Vol. 71, pp 255-265, 2004.
- [5] Franklin T. Dodge. *The new "dynamic behavior of liquids in moving containers"*. Southwest Research Institute, 2000.
- [6] Robert L. Berry and James R. Tegart. Experimental study of transient liquid motion in orbiting spacecraft. NASA, 1975.
- [7] I. Gavrilyuk, M. Hermann, I. Lukovsky, O. Solodun, A. Timokha. *Modal modeling of the fluid-structure interaction associated with sloshing in a tapered conical tank.*

Copyright Statement

The authors confirm that they, and/or their company or organization, hold copyright on all of the original material included in this paper. The authors also confirm that they have obtained permission, from the copyright holder of any third party material included in this paper, to publish it as part of their paper. The authors confirm that they give permission, or have obtained permission from the copyright holder of this paper, for the publication and distribution of this paper as part of the ICAS 2014 proceedings or as individual off-prints from the proceedings.